Thermopower of a Quantum Dot in a Coherent Regime

TAKESHI NAKANISHI[1,2] and TAKEO KATO[2]

[1] *National Institute of Advanced Industrial Science and Technology*
1 Umezono, Tsukuba 305-8568, Japan
and CREST, JST
4-1-8 Hon-machi, Kawaguchi, Saitama 332-0012, Japan
[2] *Institute for Solid State Physics, The University of Tokyo*
5-1-5 Kashiwanoha, Kashiwa, Chiba 277-8581, Japan

Thermoelectric power due to coherent electron transmission through a quantum dot is theoretically studied. In addition to the known features related to resonant peaks, we show that a novel significant structure appears between the peaks. This structure arises from the so-called transmission zero, which is characteristic of coherent transmission through several quantum levels. Because of sensitivity to the phase-breaking effect in quantum dots, this novel structure indicates the degree of coherency in the electron transmission.

KEYWORDS: thermopower, quantum dot, coherency, Aharonov-Bohm effects, conductance, Landauer formula, Mott formula

1. Introduction

Understanding electron transport through quantum dots (QDs) has been of great importance in the recent development of quantum-state engineering in semiconductor heterostructures. Although most experiments have focused on conductance, thermoelectric power (TEP) also gives useful information about the transport processes through QDs. The sequential tunneling theory predicts a sawtooth-shaped TEP oscillation as a function of gate voltage at high temperatures in a Coulomb blockade regime,[1] while cotunneling processes are expected to suppress TEP between Coulomb blockade peaks at low temperatures.[2] These predictions have been confirmed in recent experiments of QDs fabricated in two-dimensional electron gases[3–5] and single-wall carbon nanotubes.[6,7] In the previous theoretical studies of TEP, only incoherent tunneling processes have been considered. Therefore, it remains an unsolved problem how coherent electron transmission affects the TEP oscillations.

Coherent electron transport through QDs has first been revealed by conductance measurement of a QD embedded in an Aharonov-Bohm (AB) interferometer.[8–10] In the experiments, it has been shown that a transmission phase of electrons changes by π at each resonant peak in accordance with a Breit-Wigner model. This indicates that most electrons retain their coherency during the transmission through QDs.

Here, let us focus on one important feature in the experiments of the transmission phase.[8–10] A surprising and unexpected finding in these experiments is that the phase of two adjacent peaks are the same. This indicates that the transmission phase has to change by π also at another point between the peaks, even though conductance shows no detectable feature there. In order to explain this intriguing phenomenon called a 'phase lapse', a substantial body of theoretical work has been presented.[11–16] One of the key ideas for the phase lapse was proposed by Lee.[13] By general discussion based on the Friedel sum rule, he showed that vanishing of the transmission amplitude, called a transmission zero, may occur at a specific energy in quasi-1D systems with the time-reversal symmetry. He claimed that the abrupt jump of the transmission phase originates from this transmission zero. The existence of the transmission zero has been confirmed in simple noninteracting models.[14,15,17] Recently, it has been shown that the transmission zeros survive even in the presence of Coulomb interaction within the Hartree approximation.[18]

In this paper, we study TEP due to coherent electron transmission through a QD using a noninteracting model. We show that, in addition to the known TEP oscillation, a novel structure appears at the transmission zero, while no clear feature is observed in conductance there. The condition for appearance of this structure is discussed in the multilevel QD systems. We also show that this novel structure is suppressed by weak phase breaking of electrons in QDs. These features provide us with useful information about the coherency of electrons being transported through the QD.

The outline of this paper is as follows. In §2, we formulate the TEP of a QD on the basis of the Landauer formula. An artificial lead is also introduced to describe the phase breaking of electrons in the QD. In §3, we calculate TEP as a function of the chemical potential, and discuss the characteristic structures near the transmission zeros. Finally, the results are summarized in §4.

2. Thermoelectric Power of a Quantum Dot

2.1 Formulation of thermoelectric power

In a coherent regime, the conductance and TEP of mesoscopic systems are given by the Landauer formula,[3,19–25]

$$G(\mu,T) = \frac{e^2}{\pi\hbar}\int d\varepsilon T(\varepsilon)\left[-\frac{\partial f}{\partial\varepsilon}\right], \quad (2.1)$$

$$S(\mu,T) = -\frac{1}{eT}\frac{\int d\varepsilon T(\varepsilon)(\varepsilon-\mu)[-\partial f/\partial\varepsilon]}{\int d\varepsilon T(\varepsilon)[-\partial f/\partial\varepsilon]}, \quad (2.2)$$

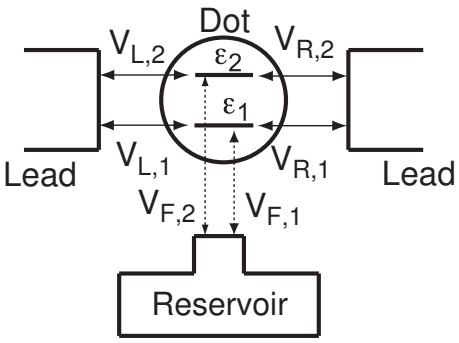

Fig. 1. A system composed of two ideal leads and a quantum dot. The reservoir connected to the dot is introduced to describe the phase-breaking effect.

with a transmission probability $T(\varepsilon)$ and a chemical potential μ in leads. Here, the derivative of a Fermi distribution function f is given by $-(\partial f/\partial\varepsilon) = (4k_BT)^{-1}\cosh^{-2}((\varepsilon-\mu)/2k_BT)$. TEP is rewritten as $S = -\langle\xi\rangle/(eT)$, where $\langle\xi\rangle$ is an average of an internal energy $\xi=\varepsilon-\mu$. Hence, TEP can be interpreted as a measure of an asymmetry in the transmission probability $T(\varepsilon)$ near the Fermi energy in the range of the thermal broadening k_BT. Here, we should note that the enhancement of TEPs is expected if transmission zeros ($T(\varepsilon) = 0$) are located near the Fermi level, because the denominator of eq. (2.2) becomes very small at low temperatures. Throughout this paper, the exact expression (2.2) is used for the calculation of TEPs.

Here, we comment on the Mott formula.[26] The Mott formula has been used widely for analysis of the TEP measurements.[3–7] It is derived by the Sommerfeld expansion of eqs. (2.1) and (2.2) up to the first order of T as

$$S_{\rm M}(\mu,T) = -\frac{\pi^2 k_{\rm B}^2 T}{3e}\frac{1}{G(\mu,T)}\frac{\partial G(\mu,T)}{\partial\mu}. \tag{2.3}$$

In the Mott formula, it is assumed that the TEP is determined only by the asymmetry of conductance at the Fermi energy. It is a good approximation as long as the product $T(\varepsilon)[-\partial f/\partial\varepsilon]$ is sufficiently large near the Fermi energy. The Mott formula is, however, not applicable to the case where the asymmetry of the product far from the Fermi level makes a significant contribution. In the present study, the Mott formula gives correct results at low temperatures, while it shows clear deviation from the exact result (2.2) at much higher temperatures than a resonant width of quantum levels in a QD. In the Appendix, we will discuss the validity of the Mott formula in detail and give a new 'extended' Mott formula, which always reproduces the correct TEP of noninteracting systems with arbitrary transmission probability $T(\varepsilon)$.

2.2 Model Hamiltonian

We study TEP in a coherent regime using the model Hamiltonian

$$H = \sum \varepsilon_{k,\alpha} C^\dagger_{k,\alpha} C_{k,\alpha} + \sum_j \varepsilon_j d^\dagger_j d_j + \sum_{k,\alpha,j} [V_{\alpha,j} C^\dagger_{k,\alpha} d_j + H.c.], \tag{2.4}$$

where operators $C_{k,\alpha}$ refer to electronic states in left ($\alpha = L$) and right ($\alpha = R$) leads, and operators d_j ($j = 1, \cdots, N$) to quantum states in the QD. In the presence of the time-reversal symmetry, we can take real coupling strengths $\{V_{\alpha,j}\}$. The model for $N = 2$ is schematically shown in Fig. 1 (the role of the reservoir will be explained in the next subsection). For this noninteracting model, the transmission coefficient can be expressed in terms of Green's function in a matrix form.[17] From the transmission coefficient, conductance eq. (2.1) and TEP eq. (2.2) are calculated by numerical integration.

2.3 Phase-breaking effect

In reality, there is always some inelastic or phase-breaking scattering. Effects of phase breaking can be studied by adding one fictitious voltage probe $\alpha = F$ connected to a reservoir.[21,22,28] Here, we only consider the two-level case ($N = 2$) with the coupling $V_{F,1} = V'$ and $V_{F,2} = V'\exp(\mathrm{i}\theta)$ (see Fig. 1). For simplicity, the phase factor θ is taken as π.[29] The chemical potential of the reservoir is determined by the condition that the current through the fictitious voltage probe vanishes. This condition is necessary to make this voltage probe play a role of simple phase breaking and to avoid other effects coming from current flow between the QD and the reservoir. Then, conductance is given by[28]

$$G = \frac{e^2}{\pi\hbar}\left[T_{RL} + \frac{T_{RF}T_{LF}}{T_{RF}+T_{LF}}\right], \tag{2.5}$$

with

$$T_{\alpha\alpha'} = \int d\varepsilon T_{\alpha\alpha'}(\varepsilon)\left[-\frac{\partial f}{\partial\varepsilon}\right], \tag{2.6}$$

where $T_{\alpha\alpha'}(\varepsilon)$ is the transmission probability from lead α' to α. For the symmetric case $T_{LF}(\varepsilon) = T_{RF}(\varepsilon)$, TEP is easily calculated with the effective transmission probability $T_{RL}+T_{LF}/2$ in eq. (2.2). Although phase breaking is considered in the minimal model, which should be improved for quantitative comparison with experiments, we can examine the crossover from a fully coherent regime to an incoherent one.

3. Results

3.1 Two-level case

We start with the two-level case ($N = 2$) for the symmetric coupling $V_{\alpha,j} = V_j$ ($j = 1, 2$) in the absence of the phase-breaking effect. The transmission coefficient is calculated as

$$t(\varepsilon) = \frac{\Gamma_1+\Gamma_2}{D}(\varepsilon-\varepsilon_0), \tag{3.1}$$

where

$$D = (\varepsilon-\varepsilon_1)(\varepsilon-\varepsilon_2) + \mathrm{i}(\Gamma_1+\Gamma_2)(\varepsilon-\varepsilon_0), \tag{3.2}$$

with $\Gamma_i = 2\pi|V_i|^2\rho$ and the density of states ρ in the leads. The transmission probability $T(\varepsilon) = |t(\varepsilon)|^2$ vanishes at a specific energy $\varepsilon_0 = (\Gamma_1\varepsilon_2+\Gamma_2\varepsilon_1)/(\Gamma_1+\Gamma_2)$ between the resonant peaks at $\varepsilon = \varepsilon_1$ and ε_2. This point is called a transmission zero.

Figure 2 shows conductance calculated for $\Gamma_1 = 2\Gamma_2 = \Gamma$ at several temperatures. Two resonant peaks with the

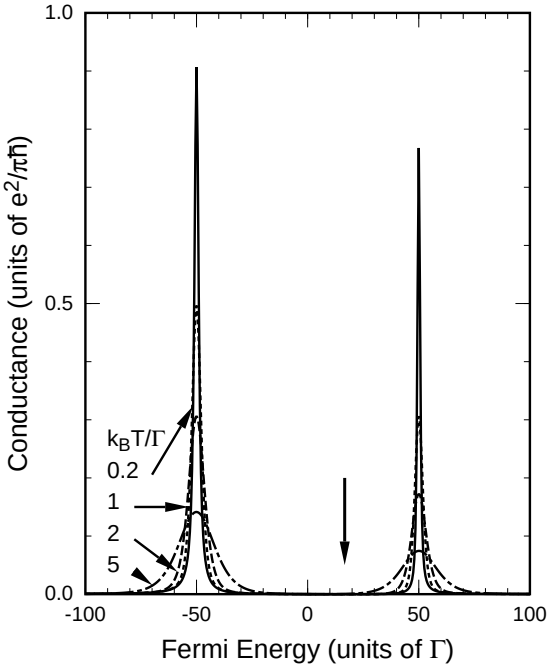

Fig. 2. Conductance with resonant peaks at $\varepsilon_1 = -50\Gamma$ and $\varepsilon_2 = 50\Gamma$ for several temperatures, $k_BT/\Gamma = 0.2$ (solid line), 1 (dotted line), 2 (dashed line), and 5 (dot-dashed line). The vertical arrow indicates the transmission zero.

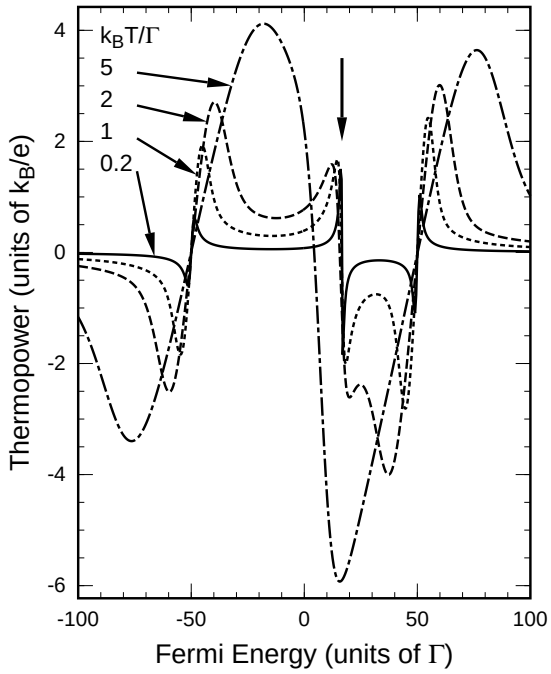

Fig. 3. Thermoelectric power for the same parameter set as that used for the conductance shown in Fig. 2. The vertical arrow indicates the transmission zero.

Breit-Wigner line shape are shown at $\varepsilon_1 = -50\Gamma$ and $\varepsilon_2 = 50\Gamma$. Although the transmission zero is located at $\mu = \varepsilon_0 = 50\Gamma/3$ (indicated by the arrow in the figure), it is not clearly seen in conductance.

TEP calculated for the same parameter set is shown in Fig. 3. Around the conductance peaks, $\varepsilon = -50\Gamma$ and $\varepsilon = 50\Gamma$, TEP shows a linear dependence on the Fermi energy with a slope $dS/d\mu = 1/(eT)$. Far from the conductance peaks, TEP deviates from this linear dependence, and decreases as the temperature decreases. These features can be understood on the basis of the sequential-tunneling and cotunneling theories[1,2] as explained in §3.3. The most unique finding is the additional sharp structure around the transmission zero ($\mu = \varepsilon_0 = 50\Gamma/3$, indicated by the arrow in the figure). We can relate this structure to the vanishing transmission amplitude as follows. By expanding the transmission amplitude around the transmission zero by $\varepsilon - \varepsilon_0$, and using the Mott formula justified at low temperatures, the TEP is obtained to be approximately

$$S_{\rm M}(\mu, T) \approx -\frac{\pi^2 k_B^2 T}{3e} \frac{2(\mu - \varepsilon_0)}{(\mu - \varepsilon_0)^2 + \pi^2 k_B^2 T^2/3}. \qquad (3.3)$$

This form fits the result shown in Fig. 3 at low temperatures. From eq. (3.3), it can be shown that TEP takes maximum and minimum values at $\mu = \varepsilon_0 \mp \pi k_{\rm B} T/\sqrt{3}$ as

$$S_{\rm Max} \approx \pm \pi k_B/\sqrt{3}e, \qquad (3.4)$$

in the low-temperature limit. For high temperature $\Gamma \ll k_{\rm B}T \ll \Delta \equiv \varepsilon_2 - \varepsilon_1$, one observes a sawtooth-like shape as predicted by the sequential tunneling theory.[1] The interference effects responsible for the transmission zero are smeared out due to the thermal broadening, and TEP vanishes at the middle point between ε_1 and ε_2 regardless of the position of the transmission zero.

Next, we replace the coupling for level 2 with an asymmetric one ($V_{\rm R,2} = -V_{\rm L,2} = V_2$) leaving level 1 symmetric ($V_{\rm L,1} = V_{\rm R,1} = V_1$). Then, the transmission coefficient becomes the difference of two Breit-Wigner line shapes as

$$t(\varepsilon) = \frac{\Gamma_1}{\varepsilon - \varepsilon_1 + {\rm i}\Gamma_1} - \frac{\Gamma_2}{\varepsilon - \varepsilon_2 + {\rm i}\Gamma_2}, \qquad (3.5)$$

and therefore the transmission amplitude never vanishes in the region between ε_1 and ε_2. Reflecting the disappearance of the transmission zero, the TEP has no structure between the resonant peaks. Thus, the appearance of the novel structure in TEP between the resonant peaks is related to the sign of the couplings.

In general, the transmission probability vanishes between the j-th and $(j+1)$-th conductance peaks for the case that the relative coupling sign, $\sigma_j \equiv {\rm sign}(V_{L,j} V_{R,j} V_{L,j+1} V_{R,j+1})$, equals +1, while no transmission zero appears for $\sigma_j = -1$.[14,15,17] Hence, the appearance of the novel structure between the j-th and $(j+1)$-th conductance peaks depends only on the relative coupling sign σ_j. We demonstrate this by studying the multilevel case in the next subsection.

3.2 Multilevel case

Figure 4 shows an example of the multilevel case at low temperature $k_BT = 0.2\Gamma$. The conductance peaks at $\varepsilon_j/\Gamma = 500(j-3)$ for $j = 1, \ldots, 5$ correspond to the levels in the QD with the couplings $V_{\alpha,1} = \sqrt{2}V$, $V_{\alpha,2} = \sqrt{5}V$, and $V_{\alpha,3} = V_{\alpha,5} = V$ for $\alpha = L, R$, while $V_{L,4} = V$ and $V_{R,4} = -V$, where $\Gamma = 2\pi|V|^2\rho$. TEP for the same parameter set shows, in addition to small spikes correspond-

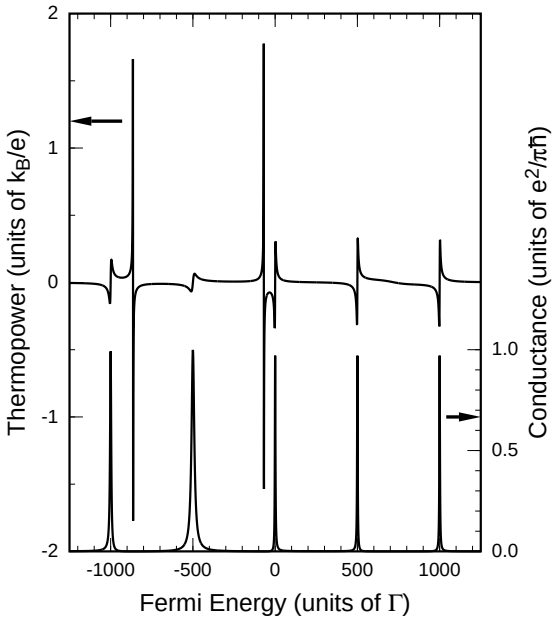

Fig. 4. Conductance and thermoelectric power of a dot with five quantum levels coupled to leads with the coupling strengths defined in the text (for $k_BT = 0.2\Gamma$).

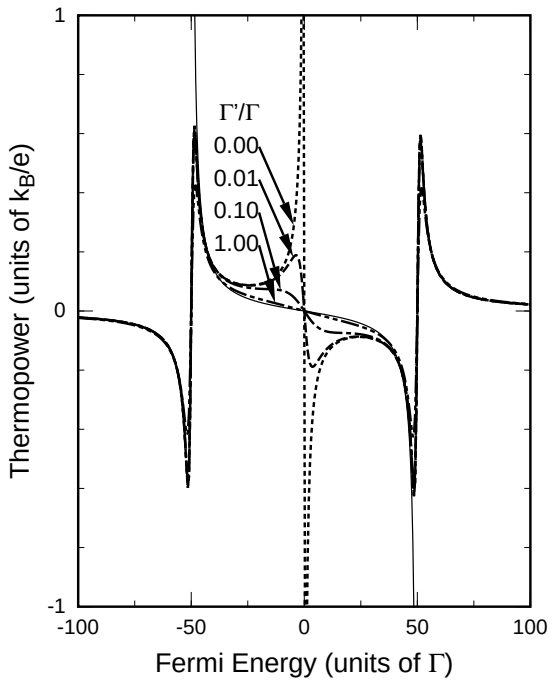

Fig. 5. Phase-breaking effect on thermoelectric power at low temperature $k_BT = 0.2\Gamma$ for several phase-breaking strengths: $\Gamma'/\Gamma = 0$ (dotted line), 0.01 (dashed line), 0.1 (dot-dashed line) and 1 (dot-dot-dashed line). The thin solid line shows the thermoelectric power predicted by the cotunneling theory (eq. (3.6)).

ing to the conductance peaks, sharp structures with an amplitude $\sim (\pi/\sqrt{3})(k_B/e)$ at the transmission zeros, $\varepsilon \sim -860\Gamma$ and -80Γ. These structures are observed between the conductance peaks of $j = 1$ and $j = 2$, and also between those of $j = 2$ and $j = 3$, because the relative coupling signs take $\sigma_j = 1$ for $j = 1, 2$. On the other hand, no sharp structure is found between other adjacent peaks, because $\sigma_j = -1$ for $j = 3, 4$. Thus, the appearance of the structures between resonant peaks can be related to the relative coupling signs, which gives the phase information of a wave function in the QD.

In general, observation of the transmission zeros in conductance measurement is rather difficult. For example, in the ordinary lead-dot-lead configuration, it is difficult to identify the transmission zeros in the region where the conductance is exponentially suppressed far from the conductance peaks. In principle, in a hybrid structure with an AB ring, the zero transmission can be detected by the abrupt jump of the transmission phase.[13] The actual analysis for this type of hybrid systems, however, is highly complicated, since the whole system consisting of a reference arm and QD should be considered as one resonator; For example, the interference within the AB ring significantly affects conductance.[12,16,27] Compared with conductance measurement, observation of the transmission zeros by using TEP may have an advantage because both measurement and analysis are simple.

3.3 Phase-breaking effect

Let us now discuss the phase-breaking effect on TEP. The strength of phase breaking can be controlled by the coupling $\Gamma' = 2\pi|V'|^2\rho'$ with the density of states ρ' in the fictitious probe. Figure 5 shows the TEP of a QD with two quantum levels ($N = 2$) for several values of Γ', where we chose $\Gamma_1 = \Gamma_2 = \Gamma$, $\varepsilon_1 = -50\Gamma$, and $\varepsilon_2 = 50\Gamma$ as a typical example. With the increase in the degree of phase breaking, the structure at the transmission zero ($\mu = \varepsilon_0 = 0$) is suppressed, because the destructive interference between two possible paths through the two levels in the QD, which is responsible for the transmission zero, is sensitively diminished by the loss of coherency. On the other hand, the small spikes corresponding to the conductance peaks are not changed so much by the phase breaking, because the conductance peak, which is determined by one dominant path through one quantum level, is insensitive to the perturbation caused by the coupling with the reservoir as long as $\Gamma' \ll \Gamma$.

For large phase breaking, it is expected that the higher-order processes with respect to the coupling $V_{\alpha,j}$ can be neglected, and that only the lowest-order ones representing the sequential-tunneling and/or cotunneling process make the main contribution. Then, the calculation in a coherent regime can be related to the known theory based on these two tunneling processes as follows.[1,2] Far from the resonant peaks, TEP is determined dominantly by the inelastic cotunneling process, which predicts the chemical-potential dependence of TEP as[2]

$$S_{\rm co} = \frac{k_B^2 T}{e}\frac{4\pi^2}{5}\left(\frac{1}{\mu-\varepsilon_1}+\frac{1}{\mu-\varepsilon_2}\right). \qquad (3.6)$$

This expression, which is drawn using the thin solid line in Fig. 5, explains well the behavior of TEP for large phase breaking except at the vicinity of the conductance peaks. The cotunneling theory breaks down near the conductance peaks, where the sequential tunneling process becomes dominant.[2] Around the conductance peaks, the slope $\mathrm{d}S/\mathrm{d}\mu = 1/(eT)$ is predicted from the sequential

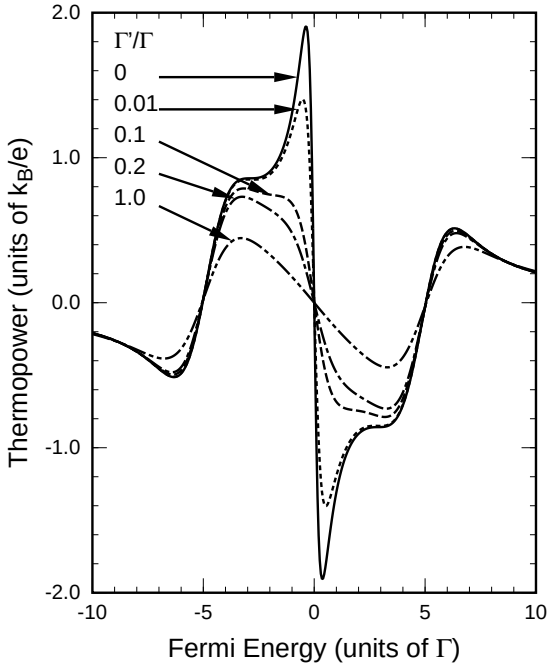

Fig. 6. Phase-breaking effect on thermoelectric power for a small level spacing $\Delta = 10\Gamma$ ($\varepsilon_1 = -5\Gamma$ and $\varepsilon_2 = 5\Gamma$) at low temperature $k_B T = 0.2\Gamma$.

tunneling theory[1] in the quantum limit $U \ll \Delta$, where U and Δ are a Coulomb interaction in the QD and a level spacing, respectively.[30] This predicted slope near the resonant peaks is consistent with all the results of TEP for weak or moderate phase breaking. For large phase breaking ($\Gamma' \gtrsim \Gamma$), the slope becomes smaller than $1/(eT)$ due to broadening of the conductance peaks.

The cotunneling theory discussed above does not work for a small level spacing Δ, where the higher-order processes are more important. We show such an example of the TEP for a small level spacing $\Delta = 10\Gamma$ ($\varepsilon_1 = -5\Gamma$ and $\varepsilon_2 = 5\Gamma$) in Fig. 6. The feature of cotunneling, which removes the structure around the transmission zero as expected from eq. (3.6), is not found even for large phase breaking, and more complicated behavior is observed. The phase breaking decreases the TEP in a wide range of the Fermi energy, while the structure at the transmission zero is suppressed by phase breaking more gradually than that for $\Delta = 100\Gamma$ in Fig. 5. This global change of TEP due to phase breaking may suggest the possibility of actual observation of electron coherency in QDs.

In order to clarify the behaviors of TEP around the transmission zero, we consider the perturbation theory with respect to the coupling $V_{\alpha,j}$. The whole transmission probability including the phase-breaking effect is evaluated around the transmission zero ($\varepsilon = 0$) up to the fourth order with respect to $V_{\alpha,j}$ as

$$T(\varepsilon) \approx \frac{8\Gamma\Gamma'}{\Delta^2} + \frac{64\Gamma(\Gamma+\Gamma')}{\Delta^4}\varepsilon^2, \qquad (3.7)$$

for $\Gamma, \Gamma' \ll \Delta$. The first term proportional to Δ^{-2} describes the incoherent cotunneling process, which leads to a finite value of the transmission amplitude at $\varepsilon = 0$. The transmission zero in coherent transport appears as a result of the destructive interference between two paths, each of which corresponds to the coherent transmission through each level in the QD. This interference process starts with the fourth order perturbation with respect to $V_{\alpha,j}$. As a result, the coherent part responsible to the transmission zero appears in the second term in eq. (3.7), and is proportional to Δ^{-4}. From the expansion (3.7), the slope of TEP at the transmission zero can be calculated at low temperatures as

$$\left.\frac{\mathrm{d}S_M}{\mathrm{d}\mu}\right|_{\mu=\varepsilon_0} \approx -\frac{k_B}{e}\left(\frac{16\pi^2 k_B T}{3\Delta^2}\left(\frac{\Gamma}{\Gamma'}+1\right)\right), \qquad (3.8)$$

which approximates well the slopes at $\mu = 0$ in Figs. 5 and 6. In the limit $\Gamma' \to \infty$, the slope agrees with that of the cotunneling theory.[2] Within this approximation, the peak height is proportional to $(k_B/e)(k_B T/\Delta)(1 + \Gamma/\Gamma')^{1/2}$ at low temperatures. Hence, a small value of Δ is preferable to observe the structure at the transmission zero.

As demonstrated so far, the structure of TEP around the transmission zero is sensitive to the phase-breaking effect. Therefore, TEP may provide a useful tool for measuring the coherency of electrons being transported through QDs. So far, the coherency of transmission electrons has been measured using the conductance of a QD embedded in an AB ring with a magnetic field. The analysis of this system is, however, complicated as discussed in §3.2. The TEP measurement, which does not need either a hybrid structure like an AB ring or an external magnetic field, may give an alternative simple method for the study of coherency in electron transport, in particular, for the off-resonant region far from the conductance peaks.

4. Summary

Thermoelectric power in a fully coherent regime has been studied theoretically. It was shown that a novel sharp structure appears at the so-called transmission zero, at which a transmission amplitude vanishes. The appearance of these structures is directly related to the sign of the coupling with leads, reflecting the phase information of wave functions in quantum dots. It was also shown that these structures are sensitively suppressed by weak phase breaking, and that the calculated thermoelectric power can be interpreted on the basis of the cotunneling theory for sufficiently large phase breaking. It was proposed that, due to sensitivity to phase breaking, thermoelectric power can be used to measure the degree of electron coherency in a quantum dot, even if the Aharonov-Bohm oscillation cannot be used due to a fairly small amplitude. The effect of Coulomb interaction on the thermoelectric power remains an important problem for future study.

Acknowledgement

We thank Y. Hamamoto for useful discussions about the derivation of the extended Mott formula, and K. Terakura for critical reading of the manuscript.

Appendix: Extended Mott Formula

The Mott formula is not applicable to the case where the asymmetry far from the Fermi energy makes an important contribution. Actually, TEP calculated with the Mott formula (2.3) clearly deviates from the exact formula (2.2) at high temperature $\Gamma \ll k_{\rm B}T \ll \Delta$ in the present study. In order to understand the deviation, we replace the transmission amplitude with one with a simple form $T(\varepsilon) = \sum_n \delta(\varepsilon - \varepsilon_n)$, where ε_n is an energy level in the QD. TEP is calculated from eq. (2.2) as $S(\mu, T) = k_{\rm B}(\mu - \varepsilon_N)/eT$, with ε_N denoting a particular ε_n closest to a given μ. On the other hand, the Mott formula gives an incorrect result $(\pi^2/3)\tanh((\mu-\varepsilon_N)/2k_{\rm B}T)$. Another example is a point contact that is almost pinched off.[31] In this case, the transmission probability is given by the step function as $T(\varepsilon) = \Theta(\varepsilon)$. TEP is calculated from eq. (2.2) as $S = (k_{\rm B}/e)\,[-\beta\mu + \ln(1-f(0))/f(0)]$, while the Mott formula (2.3) gives a different result $S_{\rm M} = (\pi^2/3)(k_{\rm B}/e)(1 - f(0))$, where $f(0) = 1/(e^{-\beta\mu}+1)$. Thus, we should use the Mott formula carefully by noting its limitation.

For general noninteracting models, we can derive an exact formula from eqs. (2.1) and (2.2) as

$$S(\mu, T) = -\frac{1}{e}\frac{1}{G(\mu, T)}\int^{\mu} d\mu' \frac{\partial G(\mu', T)}{\partial T}. \qquad \text{(A·1)}$$

This 'extended Mott formula' relates TEP to the derivative of conductance with respect to the temperature T instead of the chemical potential μ. The same relation can be rewritten in a derivative form as

$$\frac{\partial}{\partial \mu}(S(\mu, T)G(\mu, T)) = -\frac{1}{e}\frac{\partial G(\mu, T)}{\partial T}. \qquad \text{(A·2)}$$

Since this formula is always correct for noninteracting systems, it will be useful for the analysis of experimental results. On the other hand, it may become invalid in interacting electron systems. For example, the transmission probability of a carbon nanotube may depend also on the chemical potential μ when the Schottky barrier is formed at the interface between the carbon nanotube and leads. Then, a deviation from eq. (A·1) will be observed.

1) C. W. J. Beenakker and A. A. M. Staring: Phys. Rev. B **46** (1992) 9667.
2) M. Turek and K. A. Matveev: Phys. Rev. B **65** (2002) 115332.
3) H. van Houten, L. W. Molenkamp, C. W. J. Beenakker, and C. T. Foxon: Semicond. Sci. Technol. **7** (1992) B215.
4) A. S. Dzurak, C. G. Smith, C. H. W. Barnes, M. Pepper, L. Martín-Moreno, C. T. Liang, D. A. Ritchie, and G. A. C. Jones: Phys. Rev. B **55** (1997) 10197.
5) R. Scheibner, E. G. Novik, T. Borzenko, M. König, D. Reuter, A. D. Wieck, H. Buhmann, and L. W. Molenkamp: Phys. Rev. B **75** (2007) 041301.
6) J. P. Small, K. M. Perez, and P. Kim: Phys. Rev. Lett. **91** (2003) 256801.
7) M. C. Llaguno, J. E. Fisher, A. T. Johnson Jr., and J. Hone: Nano. Lett. **4** (2004) 45.
8) A. Yacoby, M. Heiblum, D. Mahalu, and H. Shtrikman: Phys. Rev. Lett. **74** (1995) 4047.
9) A. Yacoby, R. Schuster, and M. Heiblum: Phys. Rev. B **53** (1996) 9583.
10) R. Schuster, E. Buks, M. Heiblum, D. Mahalu, V. Umansky, and H. Shtrikman: Nature **385** (1997) 417.
11) G. Hackenbroich and H. A. Weidenmüller: Europhys. Lett. **38** (1997) 129.
12) J. Wu, B.-L. Gu, H. Chen, W. Duan, and Y. Kawazoe: Phys. Rev. Lett. **80** (1998) 1952.
13) H.-W. Lee: Phys. Rev. Lett. **82** (1999) 2358.
14) T. Taniguchi and M. Büttiker: Phys. Rev. B **60** (1999) 13814.
15) A. L. Yeyati and M. Büttiker: Phys. Rev. B **62** (2000) 7307.
16) A. Aharony, O. Entin-Wohlman, B. I. Halperin, and Y. Imry: Phys. Rev. B **66** (2002) 115311.
17) A. Silva, Y. Oreg, and Y. Gefen: Phys. Rev. B **66** (2002) 195316.
18) D. I. Golosov and Y. Gefen: Phys. Rev. B **74** (2006) 205316.
19) R. Landauer: IBM J. Res. Dev. **1** (1957) 223.
20) R. Landauer: Phil. Mag. **21** (1970) 863.
21) M. Büttiker: Phys. Rev. B **33** (1986) 3020.
22) M. Büttiker: IBM J. Res. Dev. **32** (1988) 63.
23) U. Sivan and Y. Imry: Phys. Rev. B **33** (1986) 551.
24) P. Streda: J. Phys. Condens. Matter **1** (1989) 1025.
25) P. N. Butcher: J. Phys. Condens. Matter **2** (1990) 4869.
26) M. Cutler and N. F. Mott: Phys. Rev. **181** (1969) 1336.
27) T. Nakanishi, K. Terakura, and T. Ando: Phys. Rev. B **69** (2004) 115307.
28) D. K. Ferry and S. M. Goodnick: *Transport in Nanostructures* (Cambridge University Press, Cambridge, 1997) p. 185.
29) The phase factor θ only changes the effective phase-breaking strength. However, we must set it with a nonzero value because the phase breaking effect disappears for $\theta = 0$ in this model.
30) We should note that, in the experiments, the opposite limit ($U \gg \Delta$) is usually realized. For this limit, we obtain the slope $\mathrm{d}S/\mathrm{d}\mu = 1/(2eT)$, which differs by a factor of 2 from the quantum limit $U \ll \Delta$.
31) A. M. Lunde and K. Flensberg: J. Phys. Condens. Matter **17** (2005) 3879.